

Optical spectroscopy of $\text{CaMoO}_4:\text{Dy}^{3+}$ single crystals

This article has been downloaded from IOPscience. Please scroll down to see the full text article.

2002 J. Phys.: Condens. Matter 14 5221

(<http://iopscience.iop.org/0953-8984/14/20/317>)

View [the table of contents for this issue](#), or go to the [journal homepage](#) for more

Download details:

IP Address: 171.66.16.104

The article was downloaded on 18/05/2010 at 06:42

Please note that [terms and conditions apply](#).

Optical spectroscopy of $\text{CaMoO}_4:\text{Dy}^{3+}$ single crystals

Enrico Cavalli¹, Enrico Bovero and Alessandro Belletti

Dipartimento di Chimica Generale ed Inorganica, Chimica Analitica e Chimica Fisica,
Università di Parma, Viale delle Scienze 17/a, 43100 Parma, Italy

E-mail: enrico.cavalli@unipr.it

Received 20 February 2002

Published 9 May 2002

Online at stacks.iop.org/JPhysCM/14/5221

Abstract

CaMoO_4 single crystals doped with Dy^{3+} were grown from sodium molybdate flux. Their absorption and visible emission spectra and decay curves were measured at different temperatures from 10 to 298 K. The complete energy level scheme has been deduced from the low-temperature measurements. The Judd–Ofelt parametrization scheme has been applied to the analysis of the room temperature absorption spectra. The calculated radiative lifetime of the $^4\text{F}_{9/2}$ state is $152 \pm 5 \mu\text{s}$, and it is in reasonable agreement with the experimental data. The decay curves measured in the 10–170 K temperature range are not exponential and obey the Inokuti–Hirayama model for energy transfer for an electric quadrupole–quadrupole interaction in the absence of diffusion among the donors. All spectral features are strongly affected by an inhomogeneous broadening connected with the ‘disordered crystal’ character of the title compound.

1. Introduction

Solid-state lasers operating in the yellow region (570–590 nm) could have important technological applications (military, telecommunication, commercial, etc). However, they have not been realized up to now because of the difficulties in finding materials suitable for this purpose. In 2000 Kaminskii *et al* [1] reported laser action of Dy^{3+} -doped tungstates in two novel laser channels, $^4\text{F}_{9/2} \rightarrow ^6\text{H}_{15/2}$ (~ 570 nm) and $^4\text{F}_{9/2} \rightarrow ^6\text{H}_{11/2}$ (~ 660 nm), at liquid nitrogen temperature under Xe-flashlamp excitation. Until then, laser action in inorganic solids activated with Dy^{3+} ions had been observed only in the NIR (1.35 and 3 μm) [2] in the case of fluoride hosts. Moreover, Dy^{3+} -doped garnets have been indicated as potential saturable absorbers in the 2.8 μm region [3]. As a consequence, the interest in the optical properties of Dy^{3+} -doped oxides is considerably increasing currently. For this reason, we have decided to undertake a study on the spectroscopic properties of a series of host lattices

¹ Author to whom any correspondence should be addressed.

activated with trivalent dysprosium. In this paper we present and discuss the optical spectra of Dy³⁺-doped calcium molybdate single crystals. CaMoO₄ belongs to the family of the tungstates and molybdates having general formula MXO₄ (M = Ca, Sr, Ba; X = W, Mo) and scheelite structure. These crystals have been reported to be good host lattices for lasing ions on one hand [2], and suitable materials for the development of Raman lasers on the other [4]. The absorption (360–1900 nm) and emission (460–850 nm) spectra and the decay curves of the luminescence were measured at temperatures ranging from 10 to 298 K. The energy level scheme for the Dy³⁺ ion in CaMoO₄ has been deduced from the low-temperature data. The intensities of the room temperature absorption bands have been analysed by means of the Judd–Ofelt (JO) theory [5, 6], and the characteristic parameters Ω_N ($N = 2, 4, 6$) and the radiative lifetime of the ⁴F_{9/2} emitting state have been evaluated. The inhomogeneous broadening of the optical features has been discussed on the basis of the ‘disordered crystal’ character arising from the substitution of Dy³⁺ for Ca²⁺ ions. Finally, the decay profiles of the luminescence have been analysed on the basis of some physical models, in order to obtain information about the excited states dynamics of the title compound.

2. Experimental details

2.1. Crystal growth and structure

CaMoO₄:Dy³⁺ single crystals were grown by means of a ‘flux growth’ method developed in our laboratory. The starting composition was: CaO 6%, Na₂CO₃ 18%, MoO₃ 75%, Dy₂O₃ 1% (in wt%). The Dy/Ca nominal ratio was 4% (molar). The mixture was put in a platinum crucible and slowly heated to 1350 °C in a horizontal furnace. After an appropriate soaking time (10–12 h) the temperature was lowered to 600 °C at a rate of 4–5 °C h⁻¹. Transparent crystals up to 3 × 2 × 1 mm³ were separated from the flux using hot diluted HCl. Their structure was checked by x-ray powder diffraction. CaMoO₄ is tetragonal, with space group *I*4₁/*a* with $a = b = 5.226$ Å and $c = 11.430$ Å, $Z = 4$ [7]. The Dy³⁺ ions occupy the Ca²⁺ sites having eightfold oxygen coordination with distorted dodecahedral geometry (the real point symmetry is S₄). This substitution requires charge compensation, that can be achieved mainly by two mechanisms:

- (a) the accommodation of Na⁺ ions arising from the growth mixture at the Ca²⁺ sites with the formation of Na⁺–Dy³⁺ pairs; and
- (b) the formation of cation vacancies.

Both mechanisms introduce disorder in the local crystal fields acting on the optically active ions. As a consequence of this so-called ‘disordered crystal’ character [2], we have to expect a marked inhomogeneous broadening of the optical features even at low temperature.

2.2. Spectroscopic measurements

The absorption and luminescence spectra and the decay curves were measured at temperatures ranging from 10 to 298 K. The absorption spectra were measured with a spectroscopic system equipped with a 300 W halogen lamp fitted with a 0.25 m Spex monochromator as source, and a 1.26 m Spex monochromator with a RCA C31034 photomultiplier, a EMI TE9684QB NIR extended photomultiplier, or a PbS NEP cell to analyse and detect the output radiation. The luminescence spectra in the visible region (440–830 nm) were measured using the same set-up with the optical pathway properly modified and a 450 W xenon lamp instead of the halogen lamp. For the measurement of the luminescence decay curves, the sample was excited at 355 nm using a pulsed Nd:YAG laser (Quanta System model SYL 202); the emission was

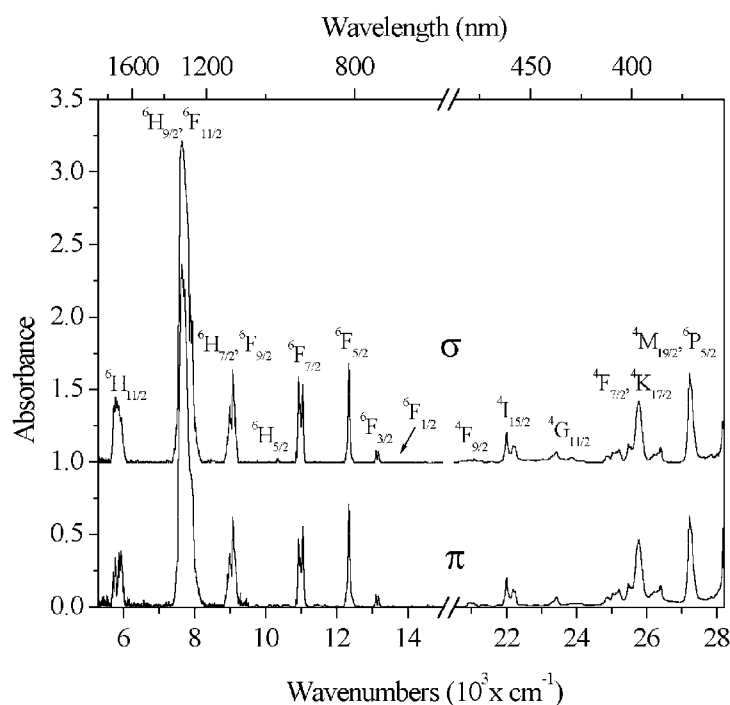


Figure 1. The 10 K polarized absorption spectrum of CaMoO₄:Dy³⁺. The thickness of the sample was 1 mm.

isolated by means of a Hilger–Watts Model D330 double monochromator and detected with a Hamamatsu R943-022 photomultiplier connected to a LeCroy 9410 transient digitizer. The samples were cooled by means of an Air Products Displex DE 202 or a Galileo Vacuum Tech Model K1 closed-cycle cryostat.

3. Absorption spectroscopy and Judd–Ofelt analysis

The 10 and 298 K absorption spectra were measured in the 360–1900 nm range using polarized light. The low-temperature ones are shown in figure 1. The observed bands have been assigned on the basis of the energy level scheme of the Dy³⁺ ion reported by several authors (see [2], for example). The high intensity of the band at 7800 cm⁻¹ can be easily explained by considering that the ${}^6F_{11/2} \leftarrow {}^6H_{15/2}$ transition is known to be hypersensitive [8]. These spectra are characterized by a strong inhomogeneous broadening of the components of the manifolds (full width at half-maximum, FWHM, of the order of 40–50 cm⁻¹), and by the nearly complete absence of polarization effects. This is a consequence of the multisite occupancy connected with the charge compensation mechanisms. The analysis of the 10 K absorption and emission spectra allows one to deduce the energy level scheme for Dy³⁺ in CaMoO₄ reported in table 1.

As expected, the bands composing the 298 K absorption spectra show a further broadening with respect to the low-temperature ones. They do not add any information about the energy level composition, and for this reason they are not shown here. Their intensities have been analysed in the framework of the JO theory. Ten bands were considered to calculate the intensity parameters Ω_N ($N = 2, 4, 6$); we did not take into account the ${}^6F_{1/2} \leftarrow {}^6H_{15/2}$ transition

Table 1. The energy level scheme of the Dy³⁺ ion in CaMoO₄.

| Level | Energy (cm ⁻¹) | Stark levels | |
|--|---|--------------|----------|
| | | Theoretical | Observed |
| ⁶ H _{15/2} | 0, 52, 165, 370, 478 | 8 | 5 |
| ⁶ H _{13/2} | 3475, 3511, 3559, 3614, 3691 | 7 | 5 |
| ⁶ H _{11/2} | 5720, 5778, 5851, 5923, 5968, 6010 | 6 | 6 |
| ⁶ H _{9/2} + ⁶ F _{11/2} | 7508, 7573, 7630, 7658, 7686, 7728, 7769, 7811, 7831, 7900, 7960 | 11 | 11 |
| ⁶ H _{7/2} + ⁶ F _{9/2} | 8936, 9001, 9030, 9082, 9174 | 9 | 5 |
| ⁶ H _{5/2} | 10254, 10330 | 3 | 2 |
| ⁶ F _{7/2} | 10940, 10979, 11054 | 4 | 3 |
| ⁶ F _{5/2} | 12345 | 3 | 1 |
| ⁶ F _{3/2} | 13116, 13182 | 2 | 2 |
| ⁶ F _{1/2} | n.o. | 1 | 1 |
| ⁴ F _{9/2} | 20921, 20973, 21008, 21070, 21317 | 5 | 5 |
| ⁴ I _{15/2} | 21958, 22017, 22085, 22202, 22252 | 8 | 5 |
| ⁴ G _{11/2} | 23266, 23310, 23430 | 6 | 3 |
| ⁴ F _{7/2} | 24863, 24912, 25038, 25138, 25214, 25484, | | |
| and upper states | 25536, 25786, 26123, 26219, 26330, 26399, 27233, 27293, 27382 | | |

Table 2. Experimental and calculated oscillator strengths (P) of Dy³⁺ in CaMoO₄. The JO parameters, Ω_λ , the RMS, and the percentage error are also tabulated. $\Omega_2 = 2.66 \times 10^{-19}$ cm², $\Omega_4 = 2.89 \times 10^{-20}$ cm², $\Omega_6 = 1.79 \times 10^{-20}$ cm², RMS = 3.74×10^{-7} ; error 7.3%.

| Excited state | Barycentre (cm ⁻¹) | P_{exp} (10 ⁶) | P_{calc} (10 ⁶) |
|--|--------------------------------|-------------------------------------|--------------------------------------|
| ⁶ H _{11/2} | 5770 | 2.92 | 2.90 |
| ⁶ H _{9/2} + ⁶ F _{11/2} | 7639 | 29.1 | 29.1 |
| ⁶ H _{7/2} + ⁶ F _{9/2} | 9051 | 3.80 | 3.71 |
| ⁶ F _{7/2} | 10974 | 2.04 | 2.49 |
| ⁶ F _{5/2} | 12370 | 1.72 | 1.04 |
| ⁶ F _{3/2} | 13142 | 0.34 | 0.19 |
| ⁴ F _{9/2} | 21014 | 0.20 | 0.19 |
| ⁴ I _{15/2} | 22099 | 1.01 | 0.94 |

because its intensity is negligible. The oscillator strengths of the transitions were carefully determined, and the experimental data were fitted on the basis of the JO parametrization scheme after subtraction of the magnetic dipole contribution for the ⁴I_{15/2} ← ⁶H_{15/2} transition. This contribution is small and not reported here. The reduced matrix elements were taken from Kaminskii [2], and the value of the refractive index was assumed to be $n = 2.0$ according to Malitson *et al* [9]. The evaluated intensity parameters are reported in table 2, together with the observed and calculated oscillator strengths, the root mean square deviation (RMS), and the percentage error. The calculated spontaneous emission probabilities and the radiative branching ratios for the transitions from the ⁴F_{9/2} state to the lower ones are reported in table 3, together with the radiative lifetime of the emitting level. They were estimated using the calculated intensity parameters and the reduced matrix elements published by Kaminskii [2] and correcting for the refractive index.

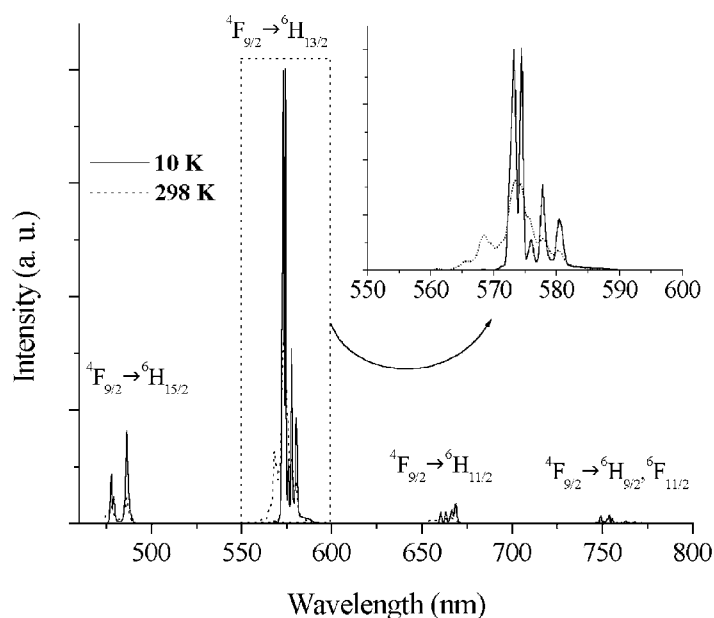


Figure 2. 10 and 298 K emission spectra of CaMoO₄:Dy³⁺.

Table 3. Calculated spontaneous emission probabilities A and radiative branching ratios β for the ${}^4F_{9/2}$ emitting level. (Radiative lifetime $\tau = 177 \mu\text{s}$.)

| Final state | A (s ⁻¹) | β |
|----------------|------------------------|---------|
| ${}^6F_{5/2}$ | 63 | 0.011 |
| ${}^6F_{7/2}$ | 13 | 0.002 |
| ${}^6H_{5/2}$ | 9 | 0.002 |
| ${}^6H_{7/2}$ | 0 | 0 |
| ${}^6F_{9/2}$ | 35 | 0.006 |
| ${}^6F_{11/2}$ | 135 | 0.024 |
| ${}^6H_{9/2}$ | 94 | 0.017 |
| ${}^6H_{11/2}$ | 530 | 0.094 |
| ${}^6H_{13/2}$ | 4412 | 0.783 |
| ${}^6H_{15/2}$ | 348 | 0.062 |

4. Emission spectroscopy and fluorescence dynamics

The 10 and 298 K emission spectra of CaMoO₄:Dy³⁺ were measured after excitation at 392 nm. They are shown in figure 2. The spectra consist of four band systems centred at about 482, 575, 666, and 755 nm. They can be assigned to the transitions from the ${}^4F_{9/2}$ level to the ${}^6H_{15/2}$, ${}^6H_{13/2}$, ${}^6H_{11/2}$, and ${}^6H_{9/2} + {}^6F_{11/2}$ states, respectively. An extremely weak band is also present at 834.8 nm, and it is assigned to the ${}^4F_{9/2} \rightarrow {}^6H_{7/2} + {}^6F_{9/2}$ transition. The ${}^4F_{9/2} \rightarrow {}^6H_{13/2}$ yellow emission gives by far the most intense band, in qualitative agreement with the results of the JO analysis presented in table 3. This band is evidenced in the inset of figure 2. As in the case of the absorption spectra, the low-temperature emission bands are affected by the inhomogeneities of the crystal fields acting on the optically active ions. As a consequence, the FWHM is never lower than 20 cm⁻¹. On passing to the room temperature spectra the band

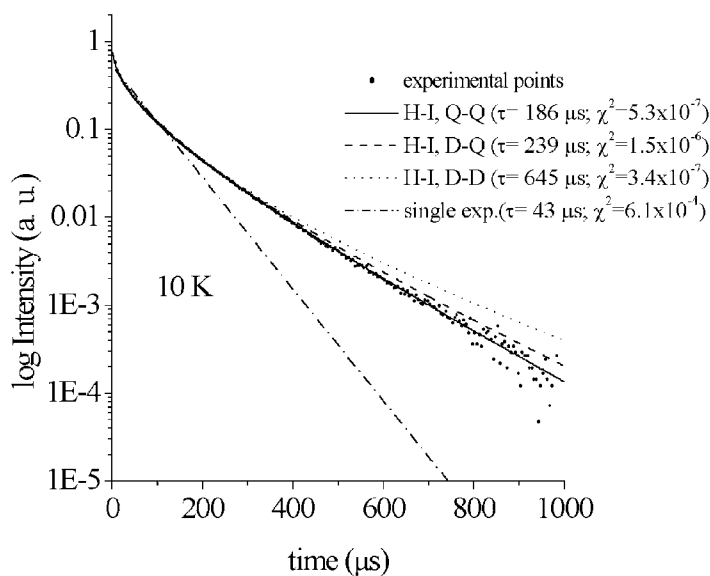


Figure 3. Results of the fit of the 10 K decay curve of the emission from the ${}^4F_{9/2}$ level. For the sake of clarity, not all of the data points have been plotted.

components broaden and tend to coalesce, giving rise, in the case of the 575 nm emission, to a single broad band ranging from 565 to 583 nm. This is an interesting behaviour because, in case of laser emission, it could imply some tunability of the output radiation.

Decay curves of the luminescence from the ${}^4F_{9/2}$ level were measured at temperatures ranging from 10 to 298 K with pulsed excitation at 355 nm. As shown by the representative example (figure 3), a single-exponential fit of the decay curves is rather unsatisfactory. The long-time tail of the decay curves has yielded a quite reliable single-exponential fit with decay times nearly independent of the temperature in the 10–170 K range. The mean value obtained, $152 \pm 5 \mu\text{s}$, is in reasonable agreement with the radiative lifetime ($177 \mu\text{s}$) evaluated by means of the JO analysis, especially if we consider the intrinsic uncertainty of the model ($\pm 20\%$) and make the reasonable assumption that the radiative lifetime does not vary significantly with the temperature. This indicates that the multiphonon relaxation is inefficient, as expected from the fact that the energy gap between the ${}^4F_{9/2}$ emitting level and the next-lower state (about 7700 cm^{-1}) is large with respect to the maximum phonon energy of the host lattice (879 cm^{-1} [4]). This agrees with the fact that it has been reported that the visible luminescence of Dy^{3+} in inorganic solids is affected by cross-relaxation, although this process has not yet been investigated thoroughly [10, 11]. To obtain more information on this topic, we have applied the Inokuti–Hirayama (IH) model [12] to the analysis of the decay curves. This model is adequate in describing energy transfer processes in which the donor–acceptor transfer is much faster than the diffusion among the donors. In the case of electric multipolar interaction the time evolution of the emission intensity from the donor is given by the following equation:

$$\phi(t) = A \exp \left[-\frac{t}{\tau} - \alpha \left(\frac{t}{\tau} \right)^{3/s} \right] \quad (1)$$

where $\phi(t)$ is the emission intensity after pulsed excitation, A is the intensity of the emission at $t = 0$, τ is the lifetime of the isolated donor, α is a parameter containing the energy transfer probability, and $s = 6$ for dipole–dipole (DD), 8 for dipole–quadrupole (DQ), and 10

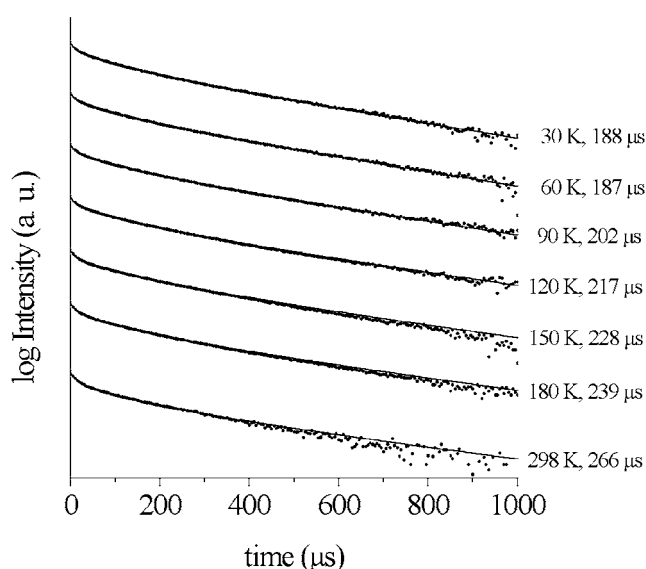
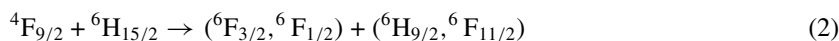


Figure 4. Decay curves and IH (QQ interaction) fits of the ${}^4F_{9/2}$ emission at different temperatures. For the sake of clarity, only some data points have been plotted.

for quadrupole–quadrupole (QQ) interactions. We have fitted the decay curves by means of equation (1) considering A , τ , and α as adjustable parameters. The three possible interaction mechanisms were taken into consideration, and the final result was that the analysis carried out with $s = 10$ has been revealed to be significantly better than those with $s = 4$ or 6 . As an example, the IH fit of the 10 K decay curve is shown in figure 3. The lifetime calculated for the case of the QQ interaction is nearly constant in the 10–60 K range, with an average value of $185 \pm 4 \mu\text{s}$; then it increases up to $230 \mu\text{s}$ at 170 K, again substantially in agreement with the radiative lifetime. This behaviour is evidenced in figure 4, where the experimental decay curves and the relative IH fits (for QQ interaction) are shown for a representative set of temperatures. Above 170 K the fit is no longer reliable. The increase of τ with the temperature has already been observed in the case of KY(MoO₄)₂:Dy and ascribed to the presence of cross-relaxation [10]. A possible process is the following:



in which the hypersensitive ${}^4F_{9/2} \rightarrow {}^6F_{11/2}$ transition is included, which follows the $\Delta J = 2$ quadrupolar selection rule [8]. The cross-relaxation process indicated is therefore consistent with the involvement of a quadrupolar mechanism. Moreover, it can be considered resonant, especially if we take into account the broadness of the transitions involved, whose origin has already been discussed.

The parameter α provides information on the probability of the energy transfer process:

$$\alpha = \frac{4}{3} \pi \Gamma \left(1 - \frac{3}{s}\right) N_a R_0^3 \quad (3)$$

where Γ is the gamma function, N_a the concentration of acceptors expressed in ions cm^{-3} , and R_0 is the critical distance. In the present case, the calculated R_0 -value ranges from 9.5 to 9.8 \AA , a reasonable value for energy transfer processes involving rare-earth ions.

The decay curves measured at temperatures higher than 170 K deviate significantly from the exponential behaviour even in their long-time tail, and the analysis based on the IH model

cannot be applied. In our opinion, this indicates that at these temperatures a number of different thermally activated energy transfer processes become efficient, possibly involving phonon-assisted energy migration in the subset of ${}^4F_{9/2}$ levels whose Stark splitting is made slightly different by the presence of disorder. For this reason, the situation probably becomes so complex that it cannot be unravelled using a simple model.

5. Conclusions

The spectroscopic properties of $\text{CaMoO}_4:\text{Dy}^{3+}$ have been investigated at different temperatures. The energy and the structure of the electronic states up to $27\,000\text{ cm}^{-1}$ have been determined on the basis of the 10 K absorption and emission spectra. The components of the observed multiplets are inhomogeneously broadened in consequence of the local disorder around the optically active ions. The JO theory has been applied to the analysis of the room temperature absorption spectra, and the intensity parameters Ω_N ($N = 2, 4, 6$) have been evaluated, together with the branching ratios and the radiative lifetime for the emission from the ${}^4F_{9/2}$ level. The comparison with the decay curves measurements, carried out at different temperatures, indicates that the multiphonon relaxation processes are ineffective, as expected on the basis of the large energy gap between the emitting and the next-lower levels. The Inokuti–Hirayama energy transfer model has been reliably applied to the analysis of the decay curves measured at temperatures ranging from 10 to 170 K. A cross-relaxation mechanism consistent with the results of this analysis was finally proposed.

Acknowledgments

The authors thank Professor M Bettinelli (Università di Verona, Italy) for helpful discussions. This work was carried out with the financial support of the Italian CNR (PF MSTAI) and MURST ('Ministero dell'Università e della Ricerca Scientifica e Tecnologica' COFIN 2001).

References

- [1] Kaminskii A A, Hömmerich U, Temple D, Seo J T, Ueda K, Bagayev S and Pavlyuk A 2000 *Japan. J. Appl. Phys.* **39** L208
- [2] Kaminskii A A 1996 *Crystalline Lasers: Physical Processes and Operating Schemes* (Boca Raton, FL: Chemical Rubber Company)
- [3] Seltzer M D, Wright A O, Morrison C A, Wortman D E, Gruber J B and Filer E D 1996 *J. Phys. Chem. Solids* **57** 1175
- [4] Basiev T T, Sobol A A, Voronko Y K and Zverev G P 2000 *Opt. Mater.* **15** 205
- [5] Judd B R 1962 *Phys. Rev.* **127** 750
- [6] Ofelt G S 1962 *J. Chem. Phys.* **37** 511
- [7] Gürmen E, Daniels E and King J S 1971 *J. Chem. Phys.* **55** 1093
- [8] Peacock R D 1975 *Structure and Bonding* vol 22 (Berlin: Springer) p 105
- [9] Malitson I H, Dodge M J, Waxler R M and Brower W S 1971 *Annual Meeting of the Optical Society of America* p 10
- [10] Hanuza J, Macalik L, Ryba-Romanowski W, Mugenski E, Cywinski R, Witke K, Piltz W and Reich P 1988 *J. Solid State Chem.* **73** 488
- [11] Macalik L, Hanuza J, Macalik B, Ryba-Romanowski W, Golab S and Pietrazko A 1988 *J. Lumin.* **79** 9
- [12] Inokuti M and Hirayama F 1965 *J. Chem. Phys.* **43** 1978